ASIAN JOURNAL OF CIVIL ENGINEERING (BUILDING AND HOUSING) VOL. 13, NO. 1 (2012)
PAGES 1-27

PREDICTION OF FAILURE PROBABILITY FOR SOIL-STRUCTURE INTERACTION SYSTEM USING MODIFIED ANFIS BY HYBRID OF FCM-FPSO

M. Khatibinia, J. Salajegheh, M.J. Fadaee and E. Salajegheh*
Department of Civil Engineering, Shahid Bahonar University of Kerman, Kerman, Iran

Received: March 2011, **Accepted:** July 2011

ABSTRACT

In this study, an efficient method is introduced to predict the stability of soil-structure interaction (SSI) system subject to earthquake loads. In the procedure of the nonlinear dynamic analysis, a number of structures collapse and then lose their stability. The prediction of failure probability is considered as stability criterion. In order to achieve this purpose, a modified adaptive neuro fuzzy inference system (ANFIS) is proposed by a hybrid of fuzzy c-means (FCM) and fuzzy particle swarm optimization (FPSO). To train the modified ANFIS, the input–output data are classified by a hybrid algorithm consisting of FCM-FPSO clustering. The optimum number of ANFIS fuzzy rules is determined by subtractive algorithm (SA). Results of illustrative examples demonstrate high performance of the modified ANFIS in comparison with the single ANFIS.

Keywords: Soil-structure interaction; failure probability; adaptive neuro fuzzy inference system; Fuzzy c-means; fuzzy particle swarm optimization; subtractive algorithm

1. INTROUDUCTION

Performance-Based Design (PBD) approach to structural design subjected to seismic loading is based on the principle that a structure should meet performance levels according to specified reliabilities over the service life [1, 2, 3]. In fact, the purpose of this approach is obtaining designs with a more predictable seismic behavior, quantifying and controlling the risk to an acceptable level. In this approach, an acceptable level of the structure depends highly on some structural parameters, some soil parameters and characteristics of earthquakes which are inherently uncertain. In order to account for possible number of these uncertainties, the reliability theory in conjunction with the PBD approach should be considered. Calculations of reliability for an acceptable level require the estimation of a number of structural responses over the duration of earthquake. These responses are

* E-mail address of the corresponding author: eysasala@mail.uk.ac.ir (E. Salajegheh)

associated with nonlinear behavior of structures, which obtained using a nonlinear dynamic analysis for each earthquake record. In procedure of the nonlinear dynamic analysis, it is probable that some of structures collapse and then lose their stability.

The problem of soil-structure interaction (SSI) is a topic of interest in engineering practice. During an earthquake, the SSI effects have an important role in determining the behavior of structures like dams, bridges, and multi-storey frames constructed on the relatively soft soil. The soft soil under structures alters the actual nonlinear dynamic behavior of structures. Thus, the interaction effects between soil and structure should be considered in the dynamic responses of structure [4, 5].

Soft computing-based models have been used in civil and structural engineering applications [6-9]. In the recent years, one of the most popular models is adaptive neuro fuzzy inference system (ANFIS) [10]. ANFIS introduced by Jang [11] is a fuzzy inference system (FIS), whose parameters of rules are tuned by artificial neural networks (ANNs). An ANFIS model depends on the number of ANFIS fuzzy rules and membership functions. In other words, an important problem for application of ANFIS in predicting problems is to determine the structure and the number of fuzzy if–then rules from an input–output data [12]. According to the FISs, ANNs tune the shape of membership functions of fuzzy variables. Thus, creating an ANFIS model with a minimum number of fuzzy rules can eliminate a well-known drawback in this model and predict data with high performance.

In this study, an efficient method is presented to train ANFIS with high performance. In the method, the main idea is to tune the shape of membership functions of fuzzy variables with the minimum number of fuzzy rules. These parameters are determined by subtractive algorithm (SA) and hybrid of fuzzy c-means (FCM) and fuzzy particle swarm optimization (FPSO). To achieve this purpose, first, the input-output data set is classified using a hybrid of FCM and FPSO. Here, the hybrid of FCM and FPSO is considered as a clustering algorithm to maintain the merits of both FCM and FPSO algorithms. The optimum number of the clusters, i.e. optimum fuzzy rules, is determined by SA. Then the number of clusters, the optimum cluster centers and membership grades of data are used in FIS to tune fuzzy parameters of ANFIS. The computational advantages of the presented method are investigated in the case of prediction of failure probability of structure subject to earthquake loads. For more detailed explanation of the proposed method, two 2D RC frames with soil under frame subjected artificial earthquakes are treated as two numerical examples. The numerical examples show the proposed method has better performance than the single ANFIS.

2. PROBABILITY OF FAILURE

Performance-based design (PBD) concept is presented to increase the safety of structures against earthquake loads. The safety of structures depends on soil and structural parameters, and characteristics of earthquakes which are inherently uncertain. This concept has presented the analytical procedures based on linear and nonlinear static and dynamic structural response for the structural analysis of buildings subjected to earthquake loading. The structural responses are applied in reliability methods which assess the structural performance. In the analysis procedure, a number of structures collapse and then lose their

stability. Theses structures should be eliminated in the assessment of structure. For this purpose, a failure probability is considered as stability criterion.

In this study, the nonlinear seismic analysis of SSI system is considered subjected to artificial earthquakes. For investigating effect of uncertain parameters, it should be considered a set of combinations of the intervening variables and parameters. First, a lower and an upper bound are chosen for each variable, and a number of combinations kept at a minimal distance apart are generated by Latin hypercube design sampling. Then, the nonlinear dynamic analysis is run for a set of combinations of the intervening variables and the failure probability is determined for these combinations.

2.1 Latin Hypercube Design Sampling

Design of computer experiments [13] is used by generating a set of combinations of the intervening variables. This set is spread in the entire space of intervening variables by design of computer experiments. In this study, Latin hypercube design (LHD) introduced by McKay *et al.* [14] for computer experiments is employed for achieving this purpose. LHD generates a Latin Hypercube Sample X containing n values on each of p variables. For each column, the n values are randomly distributed with one from each interval $(0,1/n)$, $(1/n,2/n)$,..., $(1\text{-}1/n,1)$, and they are randomly permuted. Then, it should be checked that the combinations of variables are not too close to each other. Thus, the random assignment should be repeated so that the combinations are kept at a minimal distance apart. In this study, seven peak ground accelerations (PGA) according to seismic hazard levels are selected. Using the steps of LHD sampling, 100 combinations are generated for each one of seven values for the PGA. Thus, 700 combinations are used.

2.2 Calculation of Failure Probability

For each of the 700 combinations, the steel reinforcement ratios of beams and columns should obey code requirements of ACI [15] and are sufficient to provide adequate strength for gravitational loads. For this purpose, first, the beams of structure are loaded with the combination of dead and live loads. This combination is selected according to ACI code as:

$$q_u = 1.2\,DL + 1.6\,LL \geq 1.4\,DL \tag{1}$$

where q_u, DL and LL are the uniform load on beams, dead load and live load, respectively. Then, the structure is analyzed and the code requirements of ACI for beams and columns are checked as:

$$M_u^b \leq \phi_b\, M_n^b \tag{2}$$

$$(M_u^c, P_u^c) \leq (\phi_c M_n^c, \phi_c P_n^c) \tag{3}$$

where M_u^b, M_n^b and ϕ_b are the externally applied moment due to combination of gravity loads, nominal flexural strength and strength reduction factor for beams, respectively;

$M_u^c, M_n^c, P_u^c, P_n^c$ and ϕ_c are the externally applied moment due to combination of gravity loads, nominal flexural strength subject to axial load, externally applied axial force, nominal axial strength and strength reduction factor for beams, respectively.

Also, based on ACI design code, the weak beam-strong column mechanism is considered by the following equation:

$$\frac{M_{top}^c + M_{bot}^c}{M_{left}^b + M_{right}^b} \geq 1.2 \tag{4}$$

where M_{top}^c and M_{bot}^c are the moment capacity of columns at the top and bottom of structural joint; M_{left}^b and M_{right}^b are the moment capacity of beams at the left and right of structural joint. The equation must be satisfied for all of structural joints.

Then, for each of the 700 combinations, a number of artificial earthquakes were obtained corresponding to each value of the PGA. These earthquakes were generated using different values of random phase angles. The nonlinear dynamic analysis of SSI system is run for each of sub-combinations and the responses of SSI system are obtained. In this analysis procedure, a number of sub-combinations may collapse and then lose their stability. This combination should be eliminated for these combinations. For this purpose, probability of failure, P_f, for this combination is defined as following:

$$P_f = \frac{\text{the number of collapse sub - combinations}}{\text{total of sub - combinations}} \tag{5}$$

Therefore, an efficient method should be considered to predict the failure probability. A powerful tool for this purpose is an ANFIS that modified by combining SA and hybrid of FCM and FPSO. In the next sections procedures of the method are discussed.

3. SSI SYSTEM AND ITS FINITE ELEMENT MODEL

3.1 Dynamic Inelastic SSI System

Direct method and substructure method have been proposed for modeling of SSI system. The direct method is considered in this study. In this method, discredited dynamic equations of structure and soil are considered simultaneously. Therefore, the response of the soil and structure is determined simultaneously by analyzing SSI system in each of time steps [16]. The infinite boundaries of soil containing the structure are modeled by the artificial boundaries (Figure 1).

The nonlinear discredited dynamic equation of SSI system can be formulated in the framework of the finite element method (FEM) as:

$$\boldsymbol{M}\,\Delta\ddot{\boldsymbol{u}} + \boldsymbol{C}\,\Delta\dot{\boldsymbol{u}} + \boldsymbol{K}_T\,\Delta\boldsymbol{u} = -\boldsymbol{m}_x\,\ddot{\boldsymbol{u}}_{g,x}(t+\Delta t) - \boldsymbol{F}(t) \tag{6}$$

where $\boldsymbol{M}, \boldsymbol{C}$ and $\boldsymbol{K}_T$ are the mass, damping and tangent stiffness matrices of SSI model, respectively. $\Delta\boldsymbol{u}$ is the incremental vector of the relative displacements for SSI system between times t and $t+\Delta t$. $\boldsymbol{R}(t+\Delta t)$ is the vector of the external dynamic loads at time $t+\Delta t$; and $\boldsymbol{F}(t)$ is the vector of internal forces at *t*. The term $\ddot{\boldsymbol{u}}_{g,x}(t+\Delta t)$ is the free-field components of acceleration in *x* direction, if the structure is not present. The column matrix, $\boldsymbol{m}_x$, is the directional masses for the structure only.

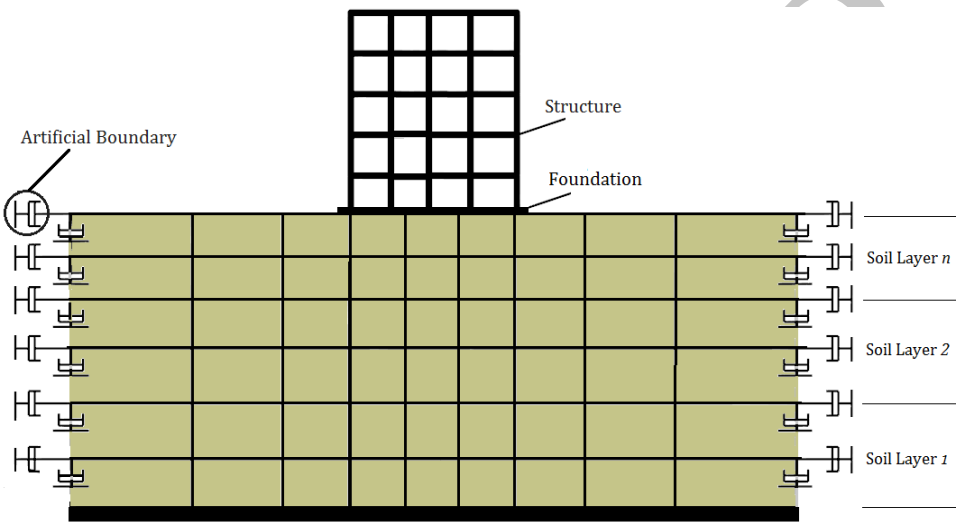

Figure 1. Modeling configuration of SSI system using direct method

The step by step time integration algorithm of Newmark [17] is used in conjunction with the following values of its constants: $\beta = 0.25, \gamma = 0.5$. Assuming that an iterative procedure is used to solve Eq. (6) over time step $[t, t+\Delta t]$ by solving a sequence of linearized problems of the form:

$$\hat{\boldsymbol{K}}_T\,\Delta\boldsymbol{u}^{i+1} = \boldsymbol{r}^i, \quad i = 1, 2, \ldots \tag{8}$$

where

$$\boldsymbol{K}^* = \boldsymbol{K}_T^i + \frac{1}{\beta(\Delta t)^2}\boldsymbol{M} + \frac{\gamma}{\beta\,\Delta t}\boldsymbol{C} \tag{9}$$

$$\boldsymbol{r}^i = -\boldsymbol{m}_x\,\ddot{\boldsymbol{u}}_{g,x}(t+\Delta t) - \boldsymbol{F}(t) - \hat{a}\,\dot{\boldsymbol{u}}_t^i - \hat{b}\,\ddot{\boldsymbol{u}}_t^i \tag{10}$$

$$\hat{a} = \frac{1}{\beta \Delta t}\boldsymbol{M} + \frac{1}{\beta}\boldsymbol{C} \; ; \; \hat{b} = \frac{1}{2\beta}\boldsymbol{M} + \Delta t(\frac{\gamma}{2\beta} - 1)\boldsymbol{C} \tag{11}$$

By solving Eq. (8), the vector of the relative displacements, $\boldsymbol{u}_{t+\Delta t}^{i+1}$, in ($i$+1)th step of the iterative procedure for SSI system is determined as.

3.2 Finite Element Model of SSI System

In this study, SSI model consists of a 2D RC frame and soil subjected to artificial earthquake excitation. The soil is layered with constant material properties along the depth. The foundation is considered as rigid strip footing. The SSI model was implemented by the finite element analysis software framework OpenSees [18]. The OpenSees is an open source object-oriented software framework for static and dynamic, linear and nonlinear finite element analysis of structural and geotechnical systems.

Beams and columns of the structure are modeled using force-based nonlinear beam column element that considers the spread of plasticity along the length of the element. The integration along the element is based on Gauss-Lobatto quadrature rule. Section stress resultants at the integration points are computed by using fibber sections with concrete and reinforcing steel material layers. The concrete material is modeled using the Kent-Scott-Park model with no tension stiffening [19]. The concrete constitutive parameters of this model are: f_c=concrete peak strength in compression; f_u=residual strength; ε_0 =strain at peak strength; and ε_u = strain at which the residual strength is reached, Figure 2(a). The constitutive behavior of the reinforcing steel is modeled using the one-dimensional J_2 plasticity model with linear hardening. The material parameters defining the J_2 plasticity model are: E=Young's modulus; f_y=yield strength; H=hardening modulus (Figure 2(b)).

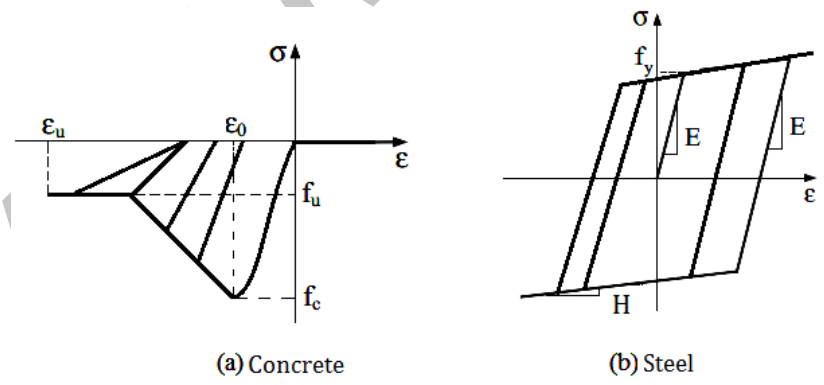

Figure 2. Material constitutive models

The soil layer is modeled using isoperimetric four-node quadrilateral finite elements with bilinear displacement interpolation. The soil domain is assumed to be under plane strain condition with a constant soil thickness, corresponding to the inter-frame distance. The soil materials are modeled using a pressure-independent multi-yield-surface J_2 plasticity model which is shown in Figure 3 [20]. The soil layer is characterized by G_i =low strain shear

modulus, B_i=bulk modulus, τ_i=shear strength, with $i=1,\ldots,n$ corresponding to the numbering of the soil layers (from bottom to top).

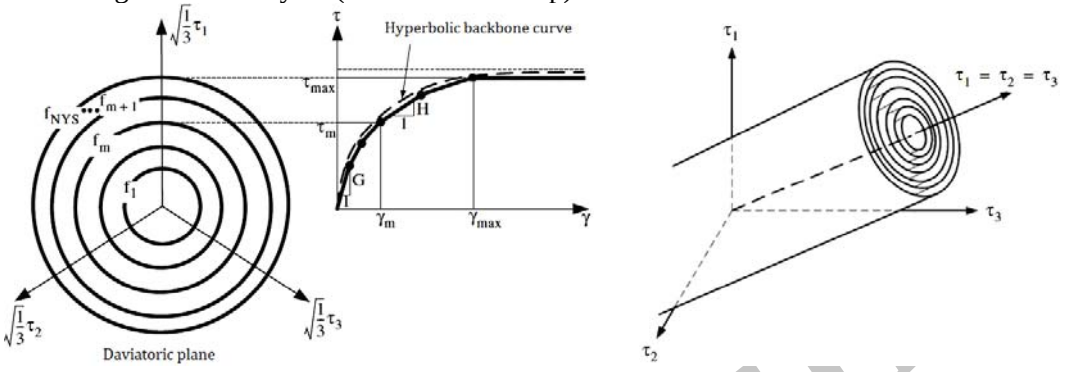

(a) Octahedral shear stress-strain (b) Von Mises multi-yield surfaces

Figure 3. Yield surfaces of multi-yield-surface J_2 plasticity model

One of the major problems in dynamic SSI system in infinite media is related to the modeling of domain boundaries. As an accurate representation of SSI system this boundary has to absorb all outgoing waves and reflect no waves back into the computational domain. One way to eliminate waves propagating outward from the structure is the standard viscous boundary, which has been proposed for the 2D case by Lysmer and Kuhlemeyer [21]. This boundary can be described by two series of dashpots oriented normal and tangential to the boundary of the FEM mesh (Figure 1) as following:

$$C_n = a\,\rho V_p \tag{12}$$

$$C_s = b\,\rho V_s \tag{13}$$

where C_n and C_s are the normal and shear damping of the boundary, respectively; ρ is the mass density of soil; a and b are dimensionless parameters to be determined, and V_p and V_s are the dilatational and shear wave velocity of propagation which are given by:

$$V_p = [\frac{2G(1-v)}{\rho(1-2v)}]^{1/2} \tag{14}$$

$$V_s = [\frac{G}{\rho}]^{1/2} \tag{15}$$

where v is Poisson ratio of soil. In this study, the standard viscous boundary improved by White *et al.* [22] with the dimensionless parameters a and b is used. The ZeroLength element is used for modeling of the standard viscous boundary with the normal and shear

damping.

The material damping matrix, $\boldsymbol{C}$, in the Eq. (6) of the SSI system is constructed by assembling the corresponding damping matrices of the structure and the soil and using the Rayleigh method [23]. The two factors of proportionality for structure and soil are computed by assuming that there is a 5% and 10% viscous damping for the structure and the soil, respectively. The $P-\Delta$ effects are considered in nonlinear time history analysis. The accelerated Newton algorithm based on Krylov subspaces [24] is applied to solving nonlinear equations of structural equilibrium.

4. ARTIFICIAL EARTHQUAKES

For seismic design of structures, either response spectrum or dynamic time history analysis subjected to earthquake is required. The dynamic time history analysis has shown its superiority both in accuracy and efficiency as compared to other methods [25]. It is then necessary to have accelerograms that has compatible characteristics and seismic excitation with desired site. Therefore, it is often difficult or may be impossible in some cases to choose a proper record for a site, because historically recorded accelerograms for the given site are scare. Hence, artificial earthquakes that are statistically influenced by desired properties of the given site are very useful for seismic design of structures. A number of approaches based on time domain and frequency domain have been proposed for the generation of synthetic ground motion records. In this paper, spectral representation method based on time domain procedure is used. The non-stationary ground motion is simulated using this method as [26]:

$$a(t) = I_m(t) \sum_{n=1}^{NFR} \{4\, S_{KT}(n\Delta f)[1+\delta_S R_N]\Delta f\}^{1/2} \sin(2\pi\, n\Delta f\, t + \theta_n) \tag{16}$$

where $a(t), I_m(t)$ and $S_{KT}(.)$ are the non-stationary ground motion, the modulation function and the specific power spectral density function (PSDF), respectively. NFR is the number of sine functions or frequencies included, between 0 and $f_{\max}$, δ_S and R_N are the coefficient of variation and a standard normal variable that used in ordinates of PSDF, Δf is frequency step, and θ_n are random phase angles with a uniform distribution between 0 and 2π. In this study, the modulation function expressed in Ref. [27] is used:

$$I_m(t) = \begin{cases} (t/T_1)^d & 0 \le t \le T_1 \\ 1 & T_1 \le t \le T_2 \\ e^{-c(t-T_2)} & T_2 \le t \le T \end{cases} \tag{17}$$

where T_1, T_2 and T are specific times and the duration of the simulated record, d and c are constants. Also, the PSDF of the non-stationary ground motion suggested by Clough and

Penzien [28] is considered as:

$$S_{KT}(f) = S_0[\frac{1+4\xi_g^2(f/f_g)^2}{(1-(f/f_g)^2)^2+4\xi_g^2(f/f_g)^2}][\frac{(f/f_f)^4}{(1-(f/f_f)^2)^2+4\xi_f^2(f/f_f)^2}] \quad (18)$$

where S_0 is the constant PSDF of input white-noise random process; f_g and ξ_g are the characteristic ground frequency and the ground damping ratio; f_f and ξ_f are parameters for a high-pass filter to attenuate low frequency components. The parameters for the generation of simulated ground motion are selected according to values that proposed by Moller *et al.* [29] as following:

Table 1: parameters for the generation of simulated ground motion

Parameter	$a_G \le 350\,cm/s^2$	$350 \le a_G \le 700\,cm/s^2$	$a_G \ge 700\,cm/s^2$
T (sec)	5.12	10.24	20.48
T_1 (sec)	0.50	1.50	2.00
T_2 (sec)	4.00	8.00	16.00
c	2.0	1.0	0.7
d	2.0	2.0	2.0
NFR	100	200	300
f_{max} (Hz)	12	15	15
δ_S	0.40	0.40	0.40

Numerical integration of artificial ground motions in the time domain often results in non-physical shifts in velocity and displacement time histories. Many methods are available to perform correction of artificial ground motion and eliminate the unrealistic velocity or displacement drift. In this paper, the method proposed by Yang *et al.* [30] is used for this purpose. The PGA values are obtained corresponding to hazard curves and produced for a specific region. In this work the hazard curves presented by Moller *et al.* [29] (Table 2) are used. An artificial earthquake generated based on Eq. (16) is shown in Figure 4.

Table 2: The PGA values of Seismic hazard levels

Probability of exceedance	**Recurrence interval**	**PGA(g)**
50% in 50 years	73	0.27
10% in 50 years	475	0.6
5% in 50 years	975	0.8

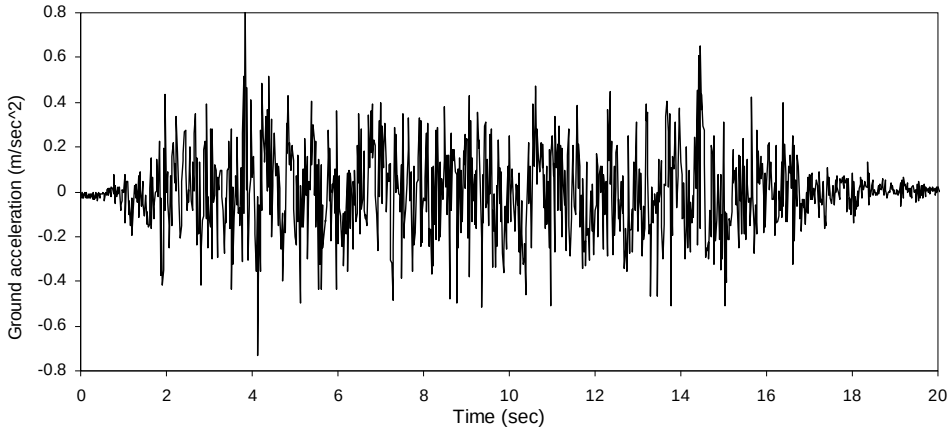

Figure 4. An artificial earthquake for PGA=0.8g

5. FUZZY C-MEANS CLUSTERING ALGORITHM

Fuzzy c-means (FCM) clustering presented by Bezdek [31] is a useful method that classified sample points into several clusters. These clusters are characterized by cluster center. Each sample point $Z = \{\boldsymbol{z}_1, \boldsymbol{z}_2, ..., \boldsymbol{z}_n\} \subset R^S$ belongs to a cluster center with a degree which is determined by the membership grade. This purpose is attained by minimizing the objective function as follow:

$$J(\boldsymbol{U}, \boldsymbol{O}) = \sum_{i=1}^{nc} \sum_{k=1}^{n} u_{ik}^{m} \left\| \boldsymbol{z}_k - \boldsymbol{o}_i \right\|_2^2 \tag{19}$$

with the constraint of

$$\sum_{i=1}^{nc} u_{ik} = 1 , \qquad k = 1, 2, \ldots, n \tag{20}$$

where $\boldsymbol{z}_k = [z_{1k}, z_{2k}, ..., z_{sk}]^T$ is an object datum, and z_{jk} is *j*th attribute value of $\boldsymbol{z}_k$; $\boldsymbol{o}_i$ is the *i*th point cluster center, and let the matrix of cluster center $\boldsymbol{O} = [o_{ji}] = [\boldsymbol{o}_1, \boldsymbol{o}_2, ..., \boldsymbol{o}_{nc}] \in R^{S \times C}$ for convenience; u_{ik} is the membership that represents the degree to which $\boldsymbol{x}_k$ belongs to the *i*th cluster, $\forall i, k : u_{ik} \in [0,1]$, and let the partition matrix $\boldsymbol{U} = [u_{ji}] \in R^{S \times C}$ for convenience; m is a fuzzification parameter, $m \in [1, \infty)$; and $\|.\|_2$ denote Euclidean norm.

In the FCM, the objective function is minimized by the Lagrange multiplier method as:

$$J_a(\boldsymbol{U}, \boldsymbol{O}) = \sum_{i=1}^{nc} \sum_{k=1}^{n} u_{ik}^{m} \left\| \boldsymbol{z}_k - \boldsymbol{o}_i \right\|_2^2 + \sum_{i=1}^{nc} \lambda_k \left(\sum_{k=1}^{n} u_{ik} - 1 \right) \tag{21}$$

where $\lambda = [\lambda_1, \lambda_2, ..., \lambda_n]^T$ is the Lagrange multiplier; and the conditions updated by

following equations are used for minimizing Eq. (19) with the constraint of Eq. (20) [31]:

$$\boldsymbol{o}_i = \frac{\sum_{k=1}^{n} u_{ik}^{m} \boldsymbol{z}_k}{\sum_{k=1}^{n} u_{ik}^{m}}, \qquad i = 1, 2, \ldots, nc \tag{22}$$

$$u_{ik} = \left[\sum_{t=1}^{nc} \left(\frac{\left\| \boldsymbol{z}_k - \boldsymbol{o}_i \right\|_2^2}{\left\| \boldsymbol{z}_k - \boldsymbol{o}_t \right\|_2^2} \right)^{\frac{1}{m-1}} \right]^{-1}, \quad i = 1, 2, \ldots, nc \; ; \; k = 1, 2, \ldots, n \tag{23}$$

The FCM algorithm is executed in the following steps:

Step 1: Choose m, nc and ε certain threshold; then initialize the partition matrix $\boldsymbol{U}^{(0)}$.

Step 2: Calculate the matrix of cluster center $\boldsymbol{O}^{(l)}$ in lth iteration using Eq. (22) and $\boldsymbol{U}^{(l-1)}$.

Step 3: Update the partition matrix $\boldsymbol{U}^{(l)}$ using Eq. (23) and $\boldsymbol{O}^{(l)}$.

Step 4: If the improvement in $J_a(\boldsymbol{U}, \boldsymbol{O})$ is less than ε, then stop and the partition matrix $\boldsymbol{U}$ and the matrix of cluster center $\boldsymbol{O}$; otherwise go to step 2.

6. FUZZY PARTICLE SWARM OPTIMIZATION FOR CLUSTERING

In FCM clustering, the objective function is nonlinear in many practical application systems, so it is difficult to optimize by using the Lagrange multiplier method. It is necessary to apply a robust optimization method, which explores the whole data space in order to reach global optimization of the problem in the data space. Recently, genetic algorithm (GA), ant colony optimization (ACO) and particle swarm optimization (PSO) have been used for clustering problems [32-34].

6.1 Particle Swarm Optimization

Particle swarm optimization (PSO) introduced by Kennedy and Eberhart [35] proved to be robust, effective and easy to apply [7, 9]. The PSO has been inspired by the social behavior of animals such as fish schooling, insects swarming and birds flocking. It involves a number of particles, which are initialized randomly in the search space of an objective function. These particles are referred to as swarm. Each particle of the swarm represents a potential solution of the optimization problem. The particle fly through the search space and its position is updated based on its velocity, the best position particle ($pbest$) and the global best position ($gbest$) that swarm has visited since the first iteration as follows:

$$\boldsymbol{V}_i^{l+1} = \omega^l \boldsymbol{V}_i^l + c_1 r_1 (\boldsymbol{pbest}_i^l - \boldsymbol{X}_i^l) + c_2 r_2 (\boldsymbol{gbest}^l - \boldsymbol{X}_i^l) \tag{24}$$

$$\boldsymbol{X}_i^{l+1} = \boldsymbol{X}_i^l + \boldsymbol{V}_i^{l+1} \tag{25}$$

where $\boldsymbol{X}_i^l$ and $\boldsymbol{V}_i^l$ represent the position and the velocity vectors of the *i*th particle in *l*th iteration, respectively; r_1 and r_2 are two uniform random sequences generated from interval [0, 1]; c_1 and c_2 are the cognitive and social scaling parameters, respectively and ω^l is the inertia weight used to discount the previous velocity of particle preserved.

6.2 Fuzzy Particle Swarm Optimization Algorithm

Mehdizadeh *et al*. [34] proposed a fuzzy particle swarm optimization (FPSO) using PSO to overcome the shortcomings of the FCM algorithm. In fact, the FPSO algorithm is developed by integrating and embedding PSO into the FCM algorithm. In FPSO, a particle represents the matrix of cluster center. In other words, the *p*th particle, $\boldsymbol{X}_p$, is expressed as follows:

$$\boldsymbol{X}_p = [\boldsymbol{o}_1, \boldsymbol{o}_2, ..., \boldsymbol{o}_{nc}] \tag{26}$$

Also, the objective function using the penalty function method is calculated as:

$$J_j(\boldsymbol{U}, \boldsymbol{O}) = \sum_{i=1}^{nc}\sum_{k=1}^{n} u_{ik}^m \left\|\boldsymbol{z}_k - \boldsymbol{o}_i\right\|_2^2 + \sum_{i=1}^{nc} \max(\sum_{k=1}^{n} u_{ik} - 1, 0), \quad j = 1, 2, ..., N_{PSO} \tag{27}$$

The FPSO algorithm is executed in the following steps:

Step 1: Choose c_1, c_2, ω, population size (N_{PSO}) and the maximum iteration $(l_{\max})$.

Step 2: Randomly initialize positions $(\boldsymbol{X}_i^0)$ and velocities $(\boldsymbol{V}_i^0)$ for $j = 1, 2, ..., N_{PSO}$.

Step 3: Update the partition matrix and calculate the objective function using Eqs. (23) and (27), respectively.

Step 4: If $J_j^{l+1} < J_{j,pbest}^l$ then $J_{j,pbest}^l = J_j^{l+1}$, $\boldsymbol{pbest}_j^{l+1} = \boldsymbol{X}_j^{l+1}$ for $j = 1, 2, ..., N_{PSO}$.

Step 5: If $\min(J_j^{l+1}) < J_{gbest}^l$ then $J_{gbest}^l = \min(J_j^{l+1})$, $\boldsymbol{gbest}^{l+1} = \boldsymbol{X}_{j,\min}^{l+1}$ for $j = 1, 2, ..., N_{PSO}$.

Step 6: Update particle velocity $\boldsymbol{V}_j^{l+1}$ and particle position $\boldsymbol{X}_j^{l+1}$ using Eqs. (24) and (25), respectively.

Step 7: If $l < l_{\max}$, then stop; otherwise go to step 3.

7. SUBTRACTIVE ALGORITHM

Subtractive algorithm (SA) is an efficient algorithm for finding the optimal number of data clusters. In SA the center candidates are the data samples themselves. So, let $Z = \{\boldsymbol{z}_1, \boldsymbol{z}_2, ..., \boldsymbol{z}_n\} \subset R^S$ be a set of *n* data samples that must be clustered. It is admitted that each of the samples defines a possible cluster center. Therefore, the potential associated to $\boldsymbol{z}_i$ is defined as follows [35]:

$$P_i(\boldsymbol{z}_i, Z) = \sum_{j=1}^{n} \exp(-\alpha \left\| \boldsymbol{z}_i - \boldsymbol{z}_j \right\|_2^2), \ \alpha = \frac{4}{r_a^2}, \ i = 1, 2, \ldots, n \tag{28}$$

where r_a is radii, a constant which defines the neighborhood radius of each point. After computing the potential for each point, the one with the highest potential is selected as the first cluster center. Next, the potential of all the remaining points is reduced as:

$$P_i = P_i - P_1^* \exp(-\beta \left\| \boldsymbol{z}_i - \boldsymbol{z}_j \right\|_2^2), \quad \beta = \frac{4}{r_b^2} \tag{29}$$

where $\boldsymbol{z}_1^*$ and P_1^* are the first group center and its potential; the constant $r_b = 1.5 r_a$ defines the neighborhood radius with sensible reductions in its potential. After performing potential reduction for all the points, the one with highest potential is selected as the second center, after what the potential of the remaining points is again reduced as:

$$P_i = P_i - P_r^* \exp(-\beta \left\| \boldsymbol{z}_i - \boldsymbol{z}_r \right\|_2^2) \tag{30}$$

The procedure of center selection and potential reduction is repeated until the stopping criterion is met. The pseudo-code of SA is as follows:

Step 1: If $P_k^* > \varepsilon^{up} P_1^*$: accept $\boldsymbol{z}_k^*$ as the next cluster center and continue

Step 2: Otherwise, if $P_k^* < \varepsilon^{down} P_1^*$: reject $\boldsymbol{z}_k^*$ and finish the algorithm

Step 3: Otherwise, let d_{min} be the shortest distance between $\boldsymbol{z}_k^*$ and all the centers already found

Step 4: If $\frac{d_{min}}{r_a} + \frac{P_k^*}{P_1^*} \geq 1$: accept $\boldsymbol{z}_k^*$ as the next cluster center and continue

Step 5: Otherwise, reject $\boldsymbol{z}_k^*$ and assign it the potential 0.0

Step 6: Select the point with higher potential as new $\boldsymbol{z}_k^*$ and repeat the process

In the above algorithm ε^{up} specifies a threshold above which the point is selected as a center with no doubts and ε^{down} specifies the threshold below which the point is definitely rejected. Typically, $\varepsilon^{up} = 0.5$, and $\varepsilon^{down} = 0.15$ [36]. It is mentioned in [37] that good values for radii are usually between 0.2 and 0.5.

8. ADAPTIVE NEURO FUZZY INTERFACE SYSTEM (ANFIS)

A fuzzy inference system (FIS) can be used as a nonlinear mapping from the input space to the output space [38]. The mapping mechanism is based on the conversion of inputs from numerical domain to fuzzy domain with using the three functional components: a rule base,

which contains a selection of fuzzy rules; a database, which defines the membership functions (MF) used in the fuzzy rules and a reasoning mechanism, which performs the inference procedure upon the rules to derive an output. ANFIS is developed by Jang [15], which is a FIS implemented in the framework of adaptive networks. For simplicity a typical ANFIS shown in Figure 5 consists of two fuzzy if–then rules based on Takagi and Sugeno's type [39]:

$$\begin{aligned} &Rule\ 1: \ \ If\ \ x\ \ is\ \ A_1\ \ and\ \ y\ \ is\ \ B_1,\ \ then\ \ f_1 = p_1x + q_1y + r_1 \\ &Rule\ 2: \ \ If\ \ x\ \ is\ \ A_2\ \ and\ \ y\ \ is\ \ B_2,\ \ then\ \ f_2 = p_2x + q_2y + r_2 \end{aligned} \tag{31}$$

where A_1, A_2, B_1 and B_2 are labels for representing MFs for the inputs x and y, respectively. Also, p_i, q_i and r_i ($i = 1, 2$) are parameters of the output MFs.

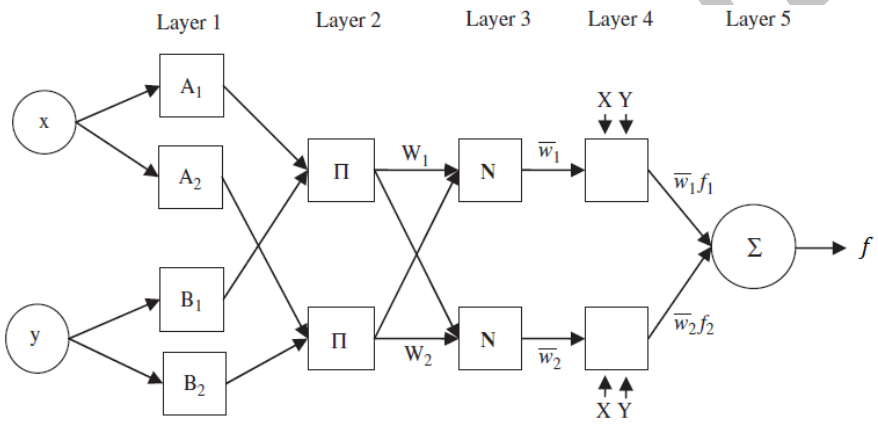

Figure 5. The architecture of ANFIS model

The general structure of ANFIS shown in Figure 5 consists of fixed square nodes and adaptive circle nodes whose parameters are changed during the training process. A hybrid learning algorithm of ANFIS is employed by the parameters of MFs of input variables and linear parameters of the output variable. These parameters are optimized using a steepest descent algorithm and a least-square method. The final output of the given network with two inputs and one output in terms of the above parameters can be calculated as follows:

$$f = \sum_i \overline{w}_i f_i = \frac{\sum_{i=1}^{2} w_i f_i}{\sum_{i=1}^{2} w_i}, \quad for\ \ i = 1, 2 \tag{32}$$

$$w_i = \mu A_i(x) \times \mu B_i(x) \quad for\ \ i = 1, 2 \tag{33}$$

where w_i is the firing strength of rule i, $\mu A_i(x)$ and $\mu B_i(x)$ are the membership degrees of x and y in A_i and B_i, respectively. Gaussian functions with maximum equal to 1 and minimum equal to 0 are selected for the membership degrees as:

$$\mu A_i(x) = \frac{1}{1+(\frac{x-c_i}{a_i})^{2b_i}} \quad (34)$$

$$\mu B_i(y) = \frac{1}{1+(\frac{y-d_i}{e_i})^{2g_i}} \quad (35)$$

where $\{a_i, b_i, c_i\}$ and $\{d_i, e_i, g_i\}$ is the premise parameter set used to adjust the shape of the membership function.

9. PROPOSED MODEL

In this study an efficient method is presented to train the failure probability with high performance. This method is a modified ANFIS by combining SA and hybrid of FCM and FPSO. The main idea is to tune the shape of membership functions of fuzzy variables with the minimum number of fuzzy rules that determined by SA and hybrid of FCM and fuzzy particle FPSO.

9.1 Hybrid of FCM and FPSO for Clustering

The FCM algorithm has been extensively studied and is known to converge to a local optimum in nonlinear problems. Moreover, the FPSO algorithm is robust method to increase the probability of achieving the global optimum in comparison with the FCM algorithm. The FCM algorithm is faster than the FPSO algorithm because it requires fewer function evaluations. This shortcoming of FPSO can be dealt with selecting an adequate initial swarm.

In this study, a hybrid clustering algorithm called FCM-FPSO is presented to use the merits of both FCM and FPSO algorithms and increase the procedure of convergence. In this way, the FCM algorithm finds an adequate initial swarm FPSO algorithm for commencing the FPSO. For this purpose, first, the FCM algorithm is employed to find a preliminary optimization that shown by $\boldsymbol{X}_{FCM}$. This optimum solution is copied N_{FCM} times to create the some part of the initial swarm FPSO. Other particles of the initial swarm, i.e. $X_{rnd,j}\ (j = 1,2,...,N_{PSO} - N_{FCM})$, are selected randomly to complete the initial swarm. Then, the FPSO algorithm is used by using this initial swarm. The algorithm flow of the FCM–FPSO strategy is shown in Figure 6.

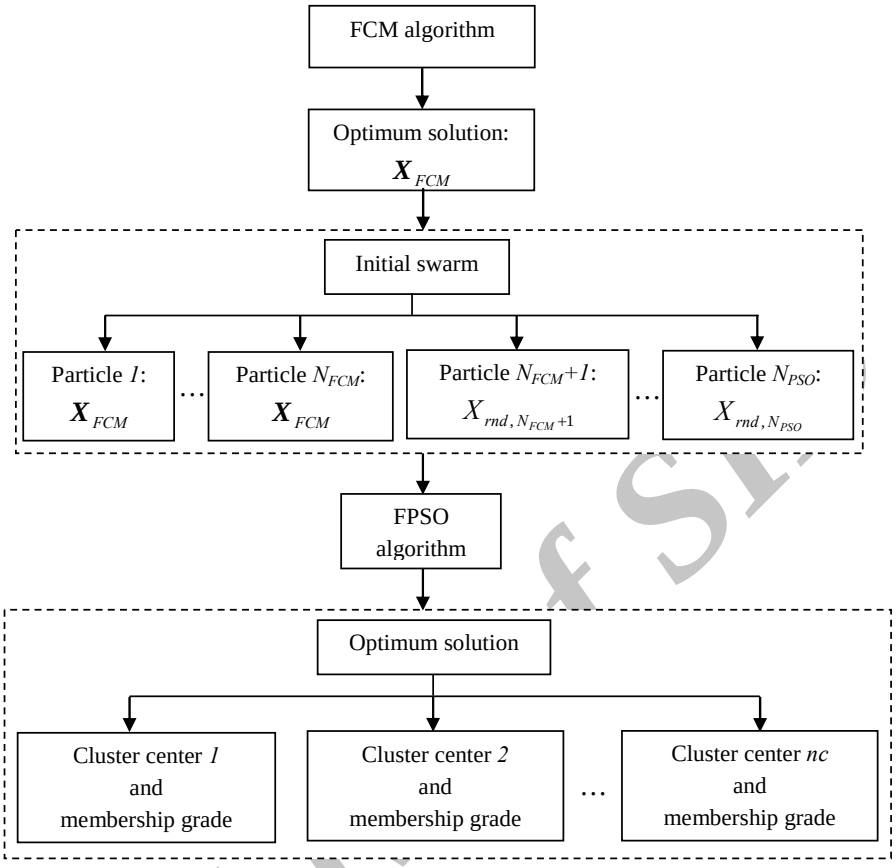

Figure 6. The algorithm flow of the FCM–FPSO for clustering

9.2 Modified ANFIS

An ANFIS model depends on the number of ANFIS fuzzy rules and membership functions. In other words, creating an ANFIS model with a minimum number of fuzzy rules can eliminate a well-known drawback. Therefore, for overcoming of this drawback, this study proposes a modified ANFIS to predict the probability of failure. In this model, the number of clusters, the cluster centers and membership grades is considered as parameters which optimized by SA and the hybrid of FCM-FPSO and used in FIS for tuning ANFIS. The algorithm flow of the proposed model is shown in Figure 7. The proposed method is executed in the following steps:

Step 1: The subtractive algorithm finds the optimum number of the clusters (*nc)*.

Step 2: The hybrid FCM-FPSO algorithm partitions training data to *nc* clusters and determines membership grades each of clusters. This parameters is used for optimizing the center of rules and membership functions for the input and output data.

Step 3: The FIS structure with a minimum number of fuzzy rules and membership functions is generated by using the SA and the hybrid FCM-FPSO algorithm. The FIS uses Gaussian function and linear function for membership function of input and output,

respectively. These parameters are tuned for the ANFIS.

Step 4: The ANFIS is employed for training data. The ANFIS uses a hybrid learning algorithm to identify parameters of Sugeno-type fuzzy inference systems. In this study, it applies a combination of the least-squares method and the backpropagation gradient descent method for training FIS membership functions.

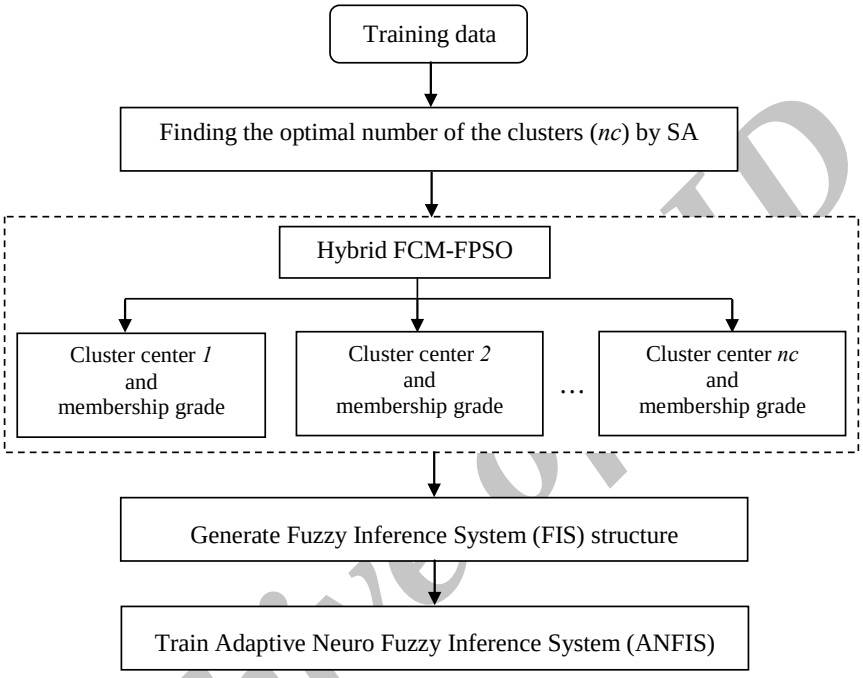

Figure 7. The algorithm flow of the proposed method

10. NUMERICAL EXAMPLES

In order to investigate the computational efficiency of the proposed method for predicting the failure probability of SSI system subject to artificial earthquakes, 2D SSI system is considered, as shown in Figure 1. The structure is a RC frame with four-bay. In the frame, the length of each bay and the height of stories are 4m and 3m, respectively. The soil consists of three-layer of sand with material properties varying along the depth. The height of each soil layer is considered 10m.

10.1 Discrete Database

The nonlinear seismic responses of SSI system depend on soil and structural parameters; and characteristics of artificial earthquakes. For investigating effect of these uncertainties, it should be considered a set of combinations of the intervening variables and parameters. First, a lower and an upper bound are chosen for each variable, and then a number of combinations kept at a minimal distance apart are generated by LHD.

As indicated in Figures 2 and 3 for nonlinear modeling of concrete, reinforcing steel and soil, the lower and upper bounds of parameters of these materials are presented in Table 3.

Table 3: Range parameters of the materials

Material	Variable	Lower bound	Upper bound
Concrete			
	$f_c\,(Mpa)$	20	35.0
	ε_u	0.003	0.004
Steel			
	$f_y\,(Mpa)$	280	400
	$E\,(Mpa)$	189×10^3	231×10^3
	H	0.019	0.021
Soil			
Layer *1*	$V_s\,(m/s)$	500	550
	ϕ	35	40
Layer *2*	$V_s\,(m/s)$	400	500
	ϕ	35	40
Layer *3*	$V_s\,(m/s)$	350	400
	ϕ	30	34

The other parameters of soil layers as B, G and V_p depend on the shear wave velocity of soil layers. For this, first, the shear wave velocity of soil layers according to their upper and lower bounds are selected, and then these parameters are calculated by the shear wave velocity.

Two cross-section databases with the lower and upper bounds and the necessary properties are generated for beams and columns that shown in Table 4. Steel reinforcement ratios of longitude bars and transverse bars followed code requirements of ACI [15] and obeyed the following ranges that indicated in Table 4. The diameter of longitudinal bars is laid between 14mm and 36mm in the databases. Columns and beams of the structure are three groups in the height of the structure.

Table 4: Range of variables for frame elements

Section	Variable	Lower bound	Upper bound
Columns			
	Width (b_C) (mm)	350	550
	Height (h_C) (mm)	350	550
	Steel reinforcement ratio (ρ_C)	1.0%	3.0%
Beams			
	Width (b_B) (mm)	250	450
	Height (h_B) (mm)	350	550
	Steel reinforcement ratio (ρ_B)	$1.4/fy$	$0.364\beta_1 f_c / f_y$

The peak ground acceleration (PGA) and the central frequency for the soil filter (f_g) is considered as the intervening variables in the generation of artificial earthquakes. Other variables for the generation of artificial earthquakes are either supposed to be functions of PGA and f_g, or supposed to be constants. The lower and upper bounds of PAG according to seismic hazard levels seismic (Table 2) and f_g are selected as shown in Table 5.

Table 5: Range of variables for the generation of artificial earthquakes

Variable	Lower bound	Upper bound
PGA (cm/s^2)	25	800
f_g (Hz)	2.0	3.0

Seven values for PGA according to Table 5 are selected. These PGA are 260, 350, 400, 550, 600, 700 and 800. Using the steps of LHD sampling, 100 combinations are generated for each one of seven values for the PGA. Thus, there are 700 combinations. For each of the 700 combinations, five artificial earthquakes were generated corresponding to each value of the PGA. The nonlinear dynamic analysis of SSI system is run for each of the five sub-combinations. For this combination the probability of failure, P_f, is calculated by Eq. (5). P_f may be 0, 0., 0.4, 0.6, 0.8 and 1. Therefore, the modified ANFIS model is employed for prediction of failure probability.

In order to validate the modified ANFIS model, this method is compared with the single ANFIS. The absolute percentage errors (*APE*) of the values of failure probability obtained by the proposed method and ANFIS in testing mode. For further comparison, relative root-

mean-squared error (*RRMSE*), mean absolute percentage error (*MAPE*) and the absolute fraction of variance (R^2) arose during testing in the proposed method and ANFIS are also calculated by using the following equations:

$$RRMSE = \sqrt{\frac{n_t \sum_{i=1}^{n_t} (a_i - p_i)^2}{(n_t - 1) \sum_{i=1}^{n_t} (a_i)^2}} \tag{35}$$

$$MAPE = \frac{1}{n_t} \sum_{i=1}^{n_t} 100 \times \left| \frac{a_i - p_i}{a_i} \right| \tag{36}$$

$$R^2 = 1 - \left(\frac{\sum_{i=1}^{n_t} (a_i - p_i)^2}{\sum_{i=1}^{n_t} p_i^2} \right) \tag{37}$$

where a is actual value, p is predicted value and n_t is number of testing sample. The smaller *RRMSE* and *MAPE* and larger R^2 mean better performance generality.

10.2 The FCM–FPSO Parameters

In order to lead the modified ANFIS to better solutions without a significant increase in the computational cost, the parameters of FCM and FPSO should be defined suitably. The appropriate values of the FCM and FPSO parameters are given in Tables 6.

Table 6: The parameter of FCM-FPSO method

Method	Parameter	Value
FCM		
	Fuzzification parameter	2.0
	Certain threshold	0.0001
FPSO		
	Particle size	50
	Social parameter	2.5
	Cognitive parameter	2.5
	Maximum iteration	100

One of the main parameters affecting the performance of the FCM–FPSO is the inertia weight (ω) in achieving efficient search behavior. The optimal inertia weight is taken as follows:

$$\omega = \omega_{\max} - \frac{\omega_{\max} - \omega_{\min}}{l_{\max}} . l \tag{38}$$

where $\omega_{\max}$ and $\omega_{\min}$ are the maximum and minimum values of ω , respectively. Also, l_{max} and l are the numbers of maximum iteration and present iteration, respectively. In this study, $\omega_{\max}$ and $\omega_{\min}$ are selected 0.09 and 0.01, respectively.

The FCM-FPSO depends on the initial FPSO particle that produced by the number of copies of the FCM solution. For this, the parameter Nc_{FCM} is defined as:

$$Nc_{FCM} = \frac{N_{FCM}}{N_{PSO}} \tag{39}$$

The value of this parameter is varied according to $Nc_{FCM} = 0.2, 0.3, 0.4$ and 0.5 while the values of other required parameters are supposed to be constant (Table 6).

The optimum number of clusters (nc) is efficient parameter in the FCM-FPSO and FISs that calculated by SA. For finding this parameter several values of r_a in the interval [0.20, 0.50] with the step of 0.005 is selected.

10.3 Example 1: A Six-Story RC Frame

In this example, six-story RC frame is considered. During the nonlinear dynamic analysis of the SSI system it is revealed that 148 combinations of database lose their stability in a number of these sub-combinations. For these combinations the probability of failure is defined according to Eq. (5). Therefore, in data set there are 148 instable and 552 stable SSI systems. In order to train the modified ANFIS, 350 samples including 100 instable and 250 stable SSI systems are considered. Also for test this method, 202 samples including 48 instable and 154 stable SSI systems are selected.

10.3.1 FCM-FPSO Algorithm

The optimal number of the clusters is found by SA. The values of 0.20 to 0.50 with the step of 0.005 have been examined for r_a and the results are given in Table 7. According to the results, it is observed that in the 62.30%, 1.64%, and 36.06% of all the cases the number of the centers found are 3, 5, and 4, respectively. Therefore, in this example the number of the centers is considered to be 3.

Table 7: The results of finding the generated data by SA.

r_a	The number of the centers found	(The centers found / all the cases)*100
0.200	3	
0.205	3	
⋮	⋮	62.30 %
0.385	3	
0.390	5	1.64 %
0.395	4	
0.400	4	
⋮	⋮	36.06 %
0.500	4	

For training samples, the FCM-FPSO algorithm partitions the data to three clusters and determines the centers of clusters and the membership grades each of clusters. The FCM-FPSO algorithm is run according to the different values of Nc_{FCM} . The average values of optimum objective function (Eq. (27)) are presented in Table 8. It is revealed that the best optimum solution is associated with Nc_{FCM} = 0.4.

Table 8: Optimum solutions obtained by FCM–FPSO for different values of Nc_{FCM}

Nc_{FCM}	0.2	0.3	0.4	0.5
Average value objective function	80.32	79.43	78.75	79.67

For the FCM, FPSO and FCM− FPSO, the convergence histories of the optimum objective function based on Eqs. (21) and (27), according to Nc_{FCM} =0.4, are shown in Figure 8.

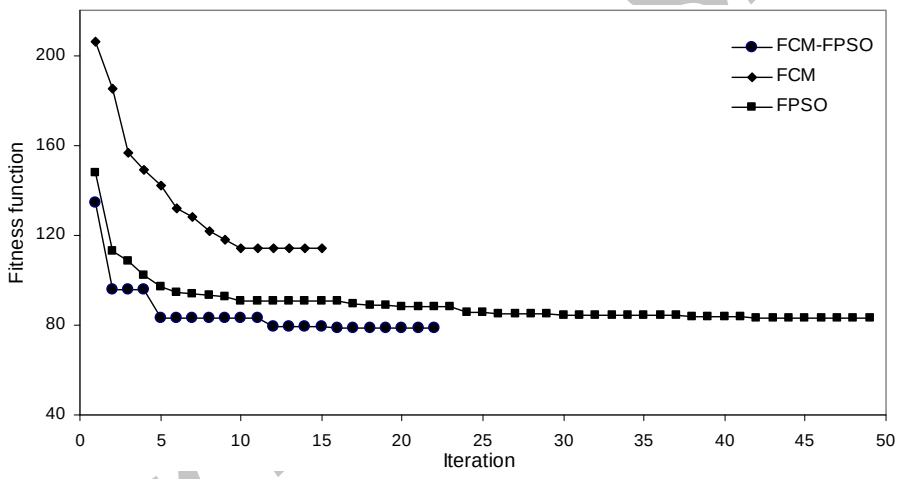

Figure 8. Convergence histories of the optimum solution of the FCM, FPSO and FCM–FPSO

10.3.2 Training and Testing the Proposed Model

The FIS structure is generated by using the optimum center of clusters and the membership grades of clusters that obtained by FCM-FPSO. In this study, the Gaussian function and linear function are used as membership function of input and output in FIS structure, respectively. The optimum number of fuzzy rules is determined by SA to be 3. This FIS is used for tuning the parameters of ANFIS. The ANFIS employs a combination of the least-squares method and the backpropagation gradient-descent method for training samples. In this study, the maximum number of epochs in training mode is set to 50. The absolute percentage errors of the design values obtained by the proposed method and ANFIS in testing mode are shown in Figure 9.

Finally, the statistical characteristics for failure probability of SSI system found from testing in the proposed method and single ANFIS are compared in Table 9. All of the statistical values in this table reveal the good performance generality of the modified ANFIS.

Table 9: Comparison of performance of the methods used based on statistical criteria

Statistical parameters	*RRMSE*	*MAPE*	R^2
The proposed method	0.1045	8.46	0.9896
ANFIS	0.1148	10.78	0.9668

As revealed in Table 9 the proposed method achieves better performance than the single ANFIS. Therefore, the proposed method is a suitable method for predicting the probability of failure.

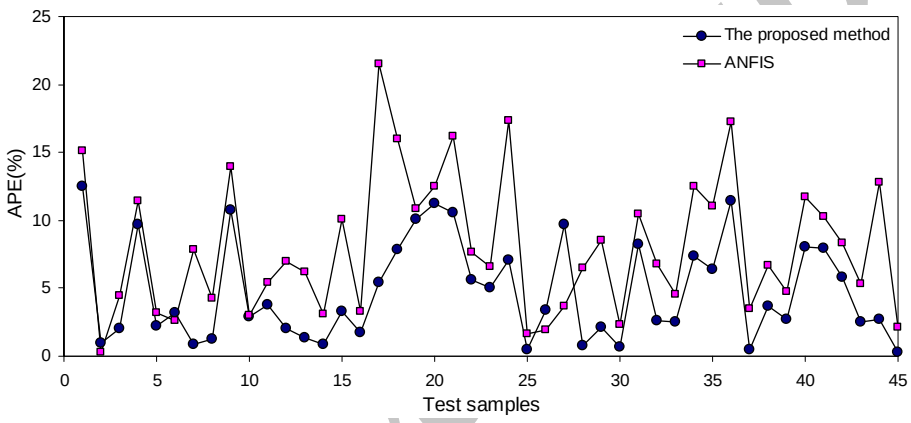

Figure 9. Absolute percentage errors

10.4 Example 2: A Nine-Story RC Frame

In this example, nine-story RC frame is considered. During the nonlinear dynamic analysis of SSI system it is revealed that 224 combinations of database lose their stability in a number of five sub-combinations. For these combinations the probability of failure is defined according to Eq. (5). Therefore, in data set there are 224 instable and 476 stable SSI systems. In order to train the modified ANFIS, 420 samples including 100 instable and 320 stable SSI systems are considered. Also for test this method, 280 samples including 124 instable and 156 stable SSI systems are selected.

10.4.1 FCM-FPSO Algorithm

According to the results of SA, it is observed that in the 55.23%, 27.48%, and 17.29% of all the cases the number of the centers found are 3, 2, and 1, respectively. Therefore, in this example the number of the centers is considered to be 3. For training samples, the FCM-FPSO algorithm partitions the data to three clusters and determines the centers of clusters and the membership grades of clusters. The FCM-FPSO algorithm is run according to the different values of Nc_{FCM}. The average values of optimum objective function (Eq. (27)) are presented in Table 10. It is revealed that the best optimum solution is associated with Nc_{FCM}= 0.3.

Table 10: Optimum solutions obtained by FCM–FPSO for different values of Nc_{FCM}

Nc_{FCM}	0.2	0.3	0.4	0.5
Average value objective function	142.02	143.76	145.17	142.75

The convergence histories of the optimum objective function based on Eqs. ((21) & (27)), according to Nc_{FCM} =0.3, are shown in Figure 10 for FCM, FPSO and FCM-FPSO.

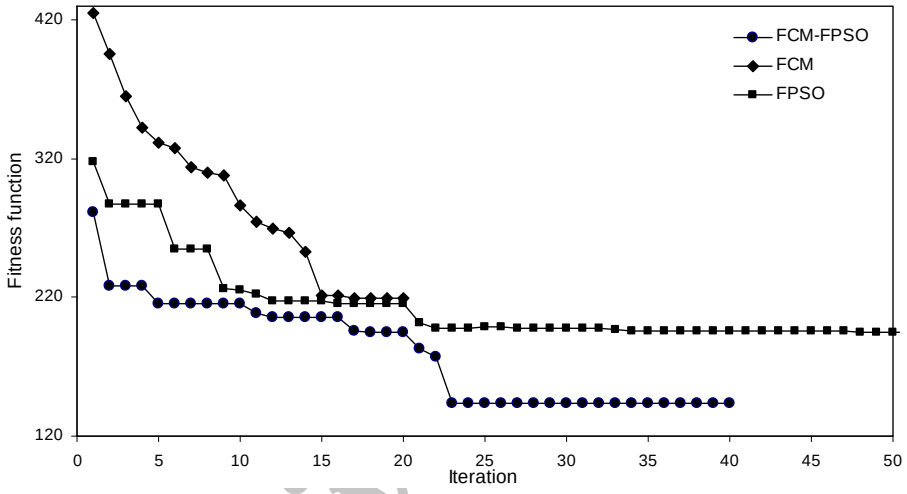

Figure 10. Convergence histories of the optimum solution of the FCM, FPSO and FCM–FPSO

10.4.2 Training and Testing the Proposed Model

The FIS structure is generated by using the optimum centers of clusters and the membership grades each of clusters that obtained by FCM-FPSO. The optimum number of fuzzy rules is determined by SA to be 3. The maximum number of epochs in training mode is set to 50. The absolute percentage errors of the design values obtained by the proposed method and ANFIS in testing mode are shown in Figure 11.

The statistical characteristics for failure probability of SSI system found from testing in the proposed method and ANFIS are compared in Table 11. All of the statistical values in this table reveal the good performance generality of the modified ANFIS.

Table 11: Comparison of performance of the methods used based on statistical criteria

Statistical parameters	*RRMSE*	*MAPE*	R^2
The proposed method	0.1012	7.21	0.9898
ANFIS	0.1575	12.68	0.9168

As revealed in Table 10 the proposed method achieves better performance than the single

ANFIS. Therefore, the proposed method is a good method for predicting the probability of failure.

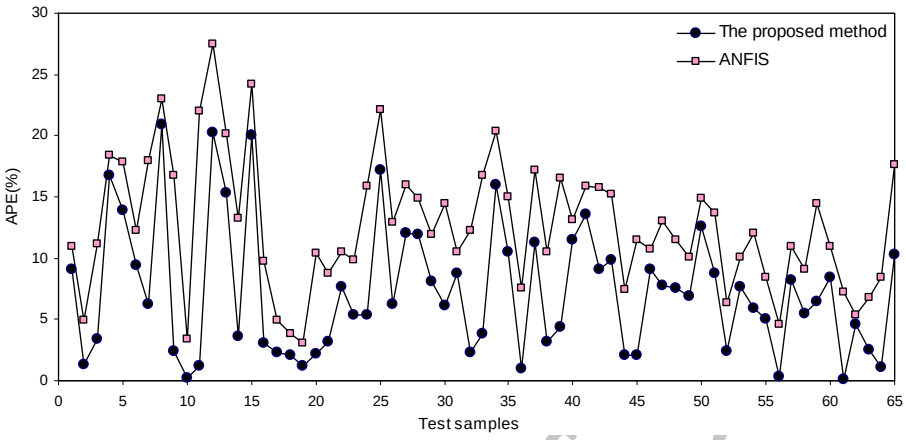

Figure 11. Absolute percentage errors

11. CONCLUSIONS

In this paper for predicting the probability of failure a modified adaptive neuro fuzzy inference system (ANFIS) is presented by a hybrid of fuzzy c-means (FCM) and fuzzy particle swarm optimization (FPSO). The accuracy of ANFIS depends on optimum number of fuzzy if–then rules and membership functions in FIS. To achieve this, subtractive algorithm (SA) and the hybrid of FCM and FPSO are employed. The main idea of hybrid of the FCM-FPSO is that combines the advantages and avoids the disadvantages of the FCM and FPSO methods. The FCM− FPSO can increase the probability of finding the global optimum, and requires lower number of iteration in the procedure optimization. Also, the FCM-FPSO can find the centers of clusters for the input and output data in FIS. The optimum number of the clusters, i.e. fuzzy rules, is determined by the SA. Numerical examples show that the proposed method has better performance generality than single ANFIS. Therefore, the proposed method can effectively predict the failure probability of soil-structure interaction (SSI) system subjected to earthquake loads.

REFERENCES

1. FEMA-356. *Prestandard and Commentary for the Seismic Rehabilitation of Buildings*, Federal Emergency Management Agency, SAC joint venture, Washington DC, 2000.
2. SEAOC vision 2000 committee. *Performance Based Seismic Engineering of Buildings*, Sacramento, California, USA: Structural Engineers Association of California, 1995.
3. Applied technology council, ATC40. Seismic Evaluation and Retrofit of Concrete Buildings California Seismic Safety Commission, 1997.

4. Mihailo DT, Maria IT, Tzong-Ying H. Full-scale experimental studies of soil–structure interaction, *ISET Journal of Earthquake Technology*, **39**(2001) 139-65.
5. John PW, Chongmin S. Some cornerstones of dynamic soil–structure interaction, *Engineering Structure*, **24**(2002) 13–28.
6. Lagaros ND, Papadrakakis M. Learning improvement of neural networks used in structural optimization, *Advances Engineering Software*, **35**(2004) 9–25.
7. Fu JY, Li QS, Xie ZN. Prediction of wind loads on a large flat roof using fuzzy neural networks, *Engineering Structure*, **28**(2006) 88–97.
8. Salajegheh E, Gholizadeh S, Khatibinia M. Optimal design of structures for earthquake loads by a hybrid RBF-BPSO method, *Earthquake Engineering and Engineering Vibration*, **7**(2008) 13-24.
9. Gholizadeh S, Salajegheh J, Salajegheh E. An intelligent neural system for predicting structural response subject to earthquakes, *Advances in Engineering Software*, **40**(2009) 630-9.
10. Salajegheh E, Salajegheh J, Seyedpoor SM, Khatibinia M. Optimal design of geometrically nonlinear space trusses using adaptive neuro-fuzzy inference system, *Scientia Iranica*, **16**(2009) 403-14.
11. Jang JS. ANFIS: adaptive-network-based fuzzy inference systems, *IEEE Transactions on Systems, Man, and Cybernetics*, **23**(1993) 665–85.
12. Angelo PP, Buswell RA. Automatic generation of fuzzy rule-based models from data by genetic algorithms, *Information Sciences*, **150**(2003) 17–31.
13. Fang KT, Li R, Sudjianto A. *Design and Modelling for Computer Experiments*, CRC Press, New York, 2006.
14. Mckay MD, Beckman RJ, Conover WJ. A comparison of three methods for selecting values on input variables in the analysis of output from a computer code, *Technometrics*, **21**(1979) 439–45.
15. American Concrete Institute (ACI 318-05), Building Code Requirements for Structural Concrete, 2005.
16. Jaya KP, Meher Prasad A. Embedded foundation in layered soil under dynamic excitations, *Soil Dynamics and Earthquake Engineering*, **22**(2002) 485–98.
17. Bathe KJ. *Finite Element Procedures*, Englewood Cliffs, Prentice-Hall, 1996.
18. OpenSees, *Open System for Earthquake Engineering Simulation*, Pacific earthquake engineering research centre, University of California, Berkeley, (Release 2.2.2), 2010. http://opensees.berkeley.edu/.
19. Kent DC, Park R. Flexural members with confined concrete, *Journal of Structural Division, ASCE*, **97**(1997) 1969-90.
20. Elgamal A, Yang Z, Parra E, Ragheb A. Modeling of cyclic mobility in saturated cohesionless soils, *International Journal of Plasticity*, **19**(2003) 883–905.
21. Lysmer J, Kuhlemeyer RL. Finite element model for infinite media, *Journal of Engineering Mechanics, ASCE*, **95**(1969) 859–77.
22. White W, Valliappan S, Lee IK. Unified boundary for finite dynamic models, *Journal of the Engineering Mechanics Division, ASCE*, **103**(1977) 949–64.
23. Chopra A. Dynamics of Structures: Theory and Applications to Earthquake Engineering, Prentice-Hall, 3nd edition, New Jersey, 2006.

24. Scott SM, Fenves GL. Krylov subspace accelerated Newton algorithm: application to dynamic progressive collapse simulation of frames, *Journal of Structure Engineering, ASCE*, **136**(2010) 473-80.
25. Atkinso G, Beresnev I. Compatible ground motion time histories for new national seismic hazard maps, *Canadian Journal of Civil Engineering*, **25**(1998) 305-18.
26. Shinozuka M, Sato Y. Simulation of nonstationary random processes. *Journal of Engineering Mechanics, ASCE*, **93**(1967) 11–40.
27. Jennings PC, Housner GW, Tasi NC. *Simulated earthquake motions*, Report, Earthquake engineering research laboratory, California Institute of Technology, 1968.
28. Clough RW, Penzien J. *Dynamics of Structures*, McGraw Hill, 1975.
29. Moller O, Foschi RO, Rubinstein M, Quiroz L. Seismic structural reliability using different nonlinear dynamic response surface approximations, *Structural Safety*, **31**(2009) 432–42.
30. Yang J, Li JB, Lin G. A simple approach to integration of acceleration data for dynamic soil–structure interaction analysis, Soil *Dynamics and Earthquake Engineering*, **26**(2006) 725–34.
31. Bezdek JC. Pattern Recognition with Fuzzy Objective Function Algorithms, Plenum Press, New York, 1981.
32. Klawonn F, Keller A. Fuzzy clustering with evolutionary algorithms, *International Journal of Intelligent Systems*, **13**(1998) 975-91.
33. Runkler TA. Ant colony optimization of clustering models, *International Journal of Intelligent Systems*, **20**(2005) 1233-61.
34. Mehdizadeh E, Sadinezhad S, Tavakkoli Moghaddam R. Optimization of fuzzy clustering criteria by a hybrid of PSO and fuzzy c-means of fuzzy clustering algorithm. *Iranian Journal of Fuzzy Systems*, **5**(2008) 1-14.
35. Kennedy J, Eberhart RC. *Swarm Intelligence*, Morgan Kaufman Publishers, 2002.
36. Paiva RP, Dourado A. Structure and parameter learning of neuro-fuzzy systems: a methodology and a comparative study, *Journal of Intelligent and Fuzzy Systems*, **11**(2001) 147–61.
37. The Language of Technical Computing. MATLAB, Math Works Inc., 2006.
38. Wang YM, Elhag T. An adaptive neuro-fuzzy inference system for bridge risk assessment, *Expert Systems with Applications*, **349**(2008) 3099-106.
39. Takagi T, Sugeno M. Derivation of fuzzy control rules from human operator's control actions, *Proceedings of IFAC Symposium on Fuzzy Information*, Knowledge Representation and Decision Analysis, 1983, pp. 55–60.